

Hydrogen Transfer to Carbonyls and Imines from a Hydroxycyclopentadienyl Ruthenium Hydride: Evidence for Concerted Hydride and Proton Transfer

Charles P. Casey,* Steven W. Singer, Douglas R. Powell, Randy K. Hayashi, and Michael Kavana

Contribution from the Department of Chemistry, University of Wisconsin, Madison, Wisconsin 53706

Received June 19, 2000. Revised Manuscript Received November 29, 2000

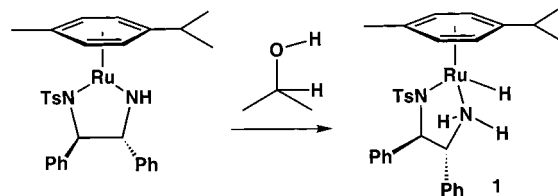
Abstract: Reaction of $\{[2,5\text{-Ph}_2\text{-}3,4\text{-Tol}_2(\eta^5\text{-C}_4\text{CO})_2\text{H}]\text{Ru}_2(\text{CO})_4(\mu\text{-H})\}$ (**6**) with H_2 formed $[2,5\text{-Ph}_2\text{-}3,4\text{-Tol}_2(\eta^5\text{-C}_4\text{COH})\text{Ru}(\text{CO})_2\text{H}]$ (**8**), the active species in catalytic carbonyl reductions developed by Shvo. Kinetic studies of the reduction of PhCHO by **8** in THF at -10°C showed second-order kinetics with $\Delta H^\ddagger = 12.0\text{ kcal mol}^{-1}$ and $\Delta S^\ddagger = -28\text{ eu}$. The rate of reduction was not accelerated by $\text{CF}_3\text{CO}_2\text{H}$, and was not inhibited by CO. Selective deuteration of the RuH and OH positions in **8** gave individual kinetic isotope effects $k_{\text{RuH}}/k_{\text{RuD}} = 1.5 \pm 0.2$ and $k_{\text{OH}}/k_{\text{OD}} = 2.2 \pm 0.1$ for PhCHO reduction at 0°C . Simultaneous deuteration of both positions in **8** gave a combined kinetic isotope effect of $k_{\text{OHRuH}}/k_{\text{ODRuD}} = 3.6 \pm 0.3$. $[2,5\text{-Ph}_2\text{-}3,4\text{-Tol}_2(\eta^5\text{-C}_4\text{COSiEt}_3)\text{Ru}(\text{CO})_2\text{H}]$ (**12**) and $\text{NEt}_4^+[2,5\text{-Ph}_2\text{-}3,4\text{-Tol}_2(\eta^5\text{-C}_4\text{CO})\text{Ru}(\text{CO})_2\text{H}]^-$ (**13**) were unreactive toward PhCHO under conditions where facile PhCHO reduction by **8** occurred. PhCOMe was reduced by **8** 30 times slower than PhCHO; MeN=CHPh was reduced by **8** 26 times faster than PhCHO. Cyclohexene was reduced to cyclohexane by **8** at 80°C only in the presence of H_2 . Concerted transfer of a proton from OH and hydride from Ru of **8** to carbonyls and imines is proposed.

Introduction

Catalytic reduction of polar functional groups mediated by transition metal complexes has emerged as a complement to stoichiometric reduction by metal hydrides such as LiAlH_4 and NaBH_4 .¹ Interest has been spurred by the development of complexes that catalyze the asymmetric reduction of ketones and imines. Chiral arene-Ru(II)-TsDPEN (*N*-(*p*-toluenesulfonyl)-1,2-diphenylethylenediamine) (**1**) catalysts reported by Noyori have achieved high levels of enantioselectivity in asymmetric transfer hydrogenations with 2-propanol as the reductant (Scheme 1).² Recent work by Mashima and Ikariya has extended Noyori's design to isoelectronic $\text{Cp}^*\text{Rh}(\text{III})$ and $\text{Cp}^*\text{Ir}(\text{III})$ -TsDPEN and TsCYDN (*N*-(*p*-toluenesulfonyl)-1,2-cyclohexadiamine) catalysts.³ In these systems, the active catalysts are proposed to be metal hydrides containing an acidic $-\text{NH}$ proton that promotes enantioselective hydrogen transfer. In the cymene-Ru and Cp^*Ir cases, these active species have been isolated and characterized. In addition, a number of groups have reported enantioselective reduction catalysts that are enhanced by an “ $-\text{NH}$ effect”, the presence of acidic amine hydrogen that is thought to enable the active hydride catalyst to achieve higher levels of selectivity and efficiency.⁴

We have had a long-standing interest in studying organometallic complexes that have acidic and hydridic hydrogens and

Scheme 1



that may function as powerful catalysts for the reduction of unsaturated organic compounds.⁵ We became intrigued by Shvo's ruthenium reduction catalyst system in which a hydroxycyclopentadienyl hydride **2**, which contains electronically coupled acidic and hydridic hydrogens, has been proposed as the active hydrogen transfer species.⁶ Shvo's catalyst system employs the diruthenium complex **3** and either H_2 or HCO_2H for the reduction of aldehydes and ketones at high temperature. **3** also catalyzed the hydrogenation of alkenes and alkynes by H_2 but not by HCO_2H . Shvo has proposed that **3** dissociates into **2** and coordinatively unsaturated dienone dicarbonyl **A**. Unsaturated intermediate **A** is proposed to react with H_2 or HCO_2H to form **2**. Shvo converted **3** to **2** at 105°C under 35 atm of H_2 or at 65°C in the presence of excess HCO_2H and showed that **2** reduces cyclohexanone to cyclohexanol at room temperature.^{6,7}

In recent work with the Shvo catalyst, Bäckvall has used **3** for the dynamic kinetic resolution of secondary alcohols. The

(1) Fehring, V.; Selke, R. *Angew. Chem., Int. Ed. Engl.* **1998**, *37*, 1827.

(2) (a) Noyori, R.; Hashiguchi, S. *Acc. Chem. Res.* **1997**, *30*, 97. (b) Haack, K.-J.; Hashiguchi, S.; Fujii, A.; Ikariya, T.; Noyori, R. *Angew. Chem., Int. Ed. Engl.* **1997**, *36*, 285. (c) Matsumura, K.; Hashiguchi, S.; Ikariya, T.; Noyori, R. *J. Am. Chem. Soc.* **1997**, *119*, 8738.

(3) (a) Mashima, K.; Abe, T.; Tani, K. *Chem. Lett.* **1998**, 1199. (b) Mashima, K.; Abe, T.; Tani, K. *Chem. Lett.* **1998**, 1201. (c) Murata, K.; Ikariya, T.; Noyori, R. *J. Org. Chem.* **1999**, *64*, 2186.

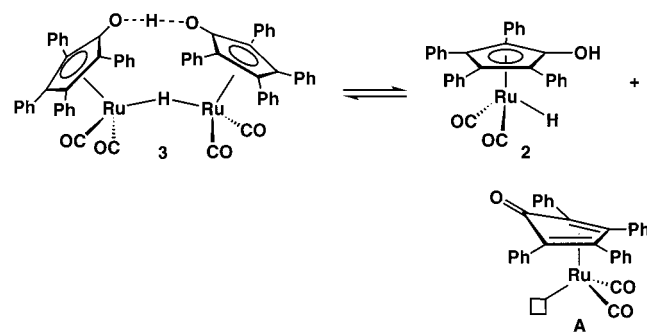
(4) For other references to transfer hydrogenation catalysts, see ref 3 in: Alonso, D. A.; Brandt, P.; Nordin, S. J. M.; Andersson, P. G. *J. Am. Chem. Soc.* **1999**, *121*, 9580.

(5) (a) Casey, C. P.; Wang, Y.; Tanke, R. S.; Hazin, P. A.; Rutter, E. W., Jr. *New J. Chem.* **1994**, *18*, 43. (b) Casey, C. P. *J. Organomet. Chem.* **1990**, *400*, 205.

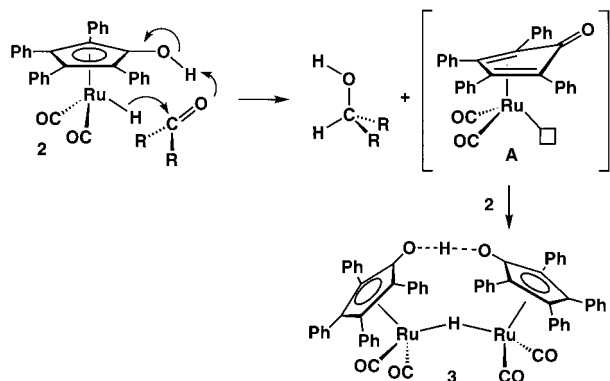
(6) Shvo, Y.; Czarkie, D.; Rahamim, Y. *J. Am. Chem. Soc.* **1986**, *108*, 7400.

(7) (a) Menashe, N.; Shvo, Y. *Organometallics* **1991**, *10*, 3885. (b) Menashe, N.; Salant, E.; Shvo, Y. *J. Organomet. Chem.* **1996**, *514*, 97.

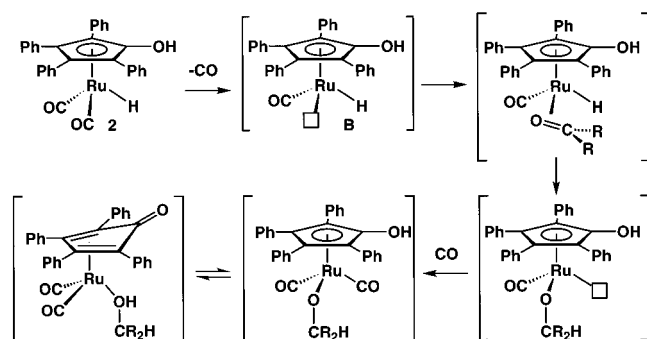
Scheme 2



Scheme 3



Scheme 4

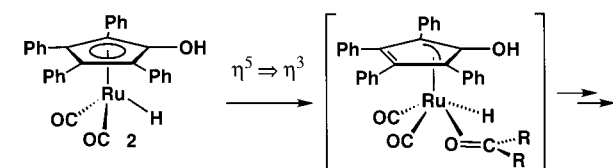


resolution exploits the ability of **3** to reversibly dehydrogenate alcohols in the presence of a lipase.⁸ The lipase selectively acylates one alcohol enantiomer while **3** racemizes the other enantiomer.

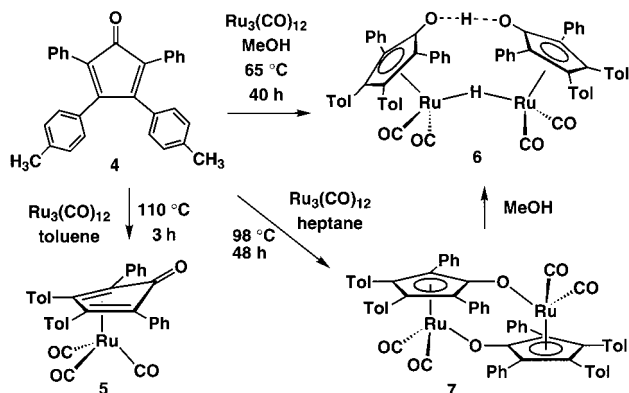
The broad scope of the Shvo catalyst and its similarity to the growing family of H^+/H^- reduction catalysts prompted us to initiate a detailed mechanistic study of the reactivity of **2** with carbonyls. At the beginning of our work, we considered three possible mechanisms for hydrogen transfer. First, simultaneous transfer of H^+ from OH and H^- from RuH might occur outside the coordination sphere of the metal (Scheme 3). Noyori has proposed a similar mechanism for reduction of ketones by the Ru(II)-TsDPEN system.^{3a}

A second possible mechanism involves CO dissociation from **2** to form the unsaturated Ru monocarbonyl hydride **B** (Scheme 4). Coordination of an aldehyde followed by intramolecular hydride addition forms an alkoxide complex.⁹ Intramolecular

Scheme 5



Scheme 6



proton transfer, CO recoordination, and alcohol dissociation complete the sequence.

A third mechanism involves η^5 - η^3 ring slippage of **2** concurrent with aldehyde complexation and subsequent intramolecular hydride addition (Scheme 5).¹⁰ Shvo has proposed that the hydrogenation of alkenes and alkynes proceeds through a ring-slip mechanism.¹¹

Here we describe detailed kinetic studies of the reduction of aldehydes, ketones, and imines by a tolyl-substituted analogue of **2**. These studies provide persuasive evidence that these reductions proceed by concerted hydrogen transfer promoted by the moderately acidic CpOH proton.

Results

Synthesis of Tolyl-Substituted Ruthenium Complexes for Mechanistic Investigations. A series of ruthenium complexes were prepared from 2,5-diphenyl-3,4-(di-*p*-tolyl)cyclopentadienone (**4**) for use in detailed mechanistic studies. The 1H NMR tolyl methyl singlets provide a convenient signature to distinguish the various ruthenium complexes.

[2,5-Ph₂-3,4-Tol₂(η^4 -C₄CO)]Ru(CO)₃ (**5**) was synthesized in 80% yield by heating $Ru_3(CO)_{12}$ and 2,5-diphenyl-3,4-(di-*p*-tolyl)cyclopentadienone (**4**) in refluxing toluene (Scheme 6). Dienone tricarbonyl complex **5** had spectroscopic features very similar to those reported for the tetraphenyl analogue.¹² The 1H NMR resonance for the tolyl methyl group was observed at δ 1.82.

{[2,5-Ph₂-3,4-Tol₂(η^5 -C₄CO)]₂H}Ru₂(CO)₄(μ -H) (**6**). By using a procedure similar to that reported by Shvo for **3**, treatment of cyclopentadienone ruthenium complex **5** with

(9) Gladysz has studied related σ - and π -aldehyde rhenium complexes. (a) Garner, C. M.; Méndez, N. Q.; Kowalczyk, J. J.; Fernández, J. M.; Emerson, K.; Larsen, R. D.; Gladysz, J. A. *J. Am. Chem. Soc.* **1990**, *112*, 5146. (b) Méndez, N. Q.; Mayne, C. L.; Gladysz, J. A. *Angew. Chem., Int. Ed. Engl.* **1990**, *29*, 1475. (c) Méndez, N. Q.; Arif, A. M.; Gladysz, J. A. *Angew. Chem., Int. Ed. Engl.* **1990**, *29*, 1473.

(10) The hydroxycyclopentadienyl ligand can ring slip in three directions, but only the symmetric ring slip is shown.

(11) Shvo, Y.; Goldberg, I.; Czerkic, D.; Reshef, D.; Stein, Z. *Organometallics* **1997**, *16*, 133.

(12) (a) Bruce, M. I.; Knight, J. R. *J. Organomet. Chem.* **1968**, *12*, 411. (b) Bailey, N. A.; Jassal, V. S.; Vefghi, R.; White, C. J. *Chem. Soc., Dalton Trans.* **1987**, 2815.

(8) (a) Larsson, A. L. E.; Persson, B. A.; Bäckvall, J. E. *Angew. Chem., Int. Ed. Engl.* **1997**, *36*, 1211. (b) Persson, B. A.; Larsson, A. L. E.; Le Ray, M.; Bäckvall, J. E. *J. Am. Chem. Soc.* **1999**, *121*, 1645. (c) Persson, B. A.; Huerta, F. F.; Bäckvall, J. E. *J. Org. Chem.* **1999**, *64*, 5237. (d) Huerta, F. F.; Laxmi, Y. R. S.; Bäckvall, J. E. *Org. Lett.* **2000**, *2*, 1037. (e) Laxmi, Y. R. S.; Bäckvall, J. E. *Chem. Commun.* **2000**, 611.

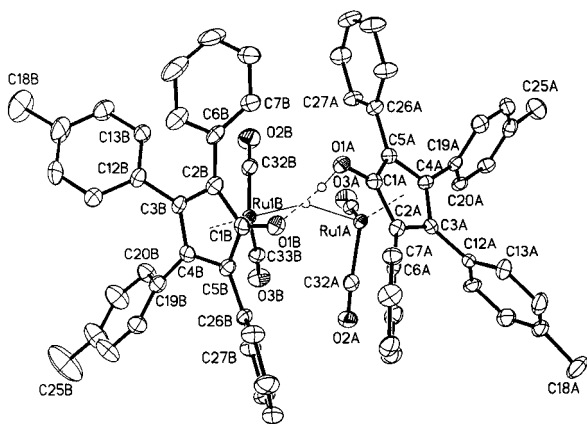


Figure 1. X-ray Crystal Structure of $\{[2,5\text{-Ph}_2\text{-3,4-Tol}_2(\eta^5\text{-C}_4\text{CO})]_2\text{H}\}\text{-Ru}_2(\text{CO})_4(\mu\text{-H})$ (**6**). Thermal ellipsoids are drawn at 50% probability.

Na_2CO_3 in acetone gave a 50% yield of diruthenium complex **6**. We developed a more convenient and more efficient one-step procedure for the synthesis of **6**. Refluxing $\text{Ru}_3(\text{CO})_{12}$ and cyclopentadienone **4** in CH_3OH for 40 h produced a 59% yield of **6** as a pure yellow precipitate (Scheme 6). In the ^1H NMR spectrum of **6** in C_6D_6 , the bridging hydride resonance appeared at $\delta -17.68$ and the bridging hydroxyl resonance appeared as a broad singlet at $\delta 12.90$.⁶ Addition of D_2O led to a greatly diminished intensity of the $\delta 12.90$ resonance due to OH/OD exchange.

In the X-ray crystal structure of **6** (Figure 1), the $\text{Ru}(1)\text{-C}(1)$ bond length of 2.40 \AA and the $\text{C}(1)\text{-O}(1)$ bond length of 1.29 \AA provide evidence for η^5 -coordination of the cyclopentadienyl ligands.¹³ The two $\text{Ru}(\text{CO})_2$ units are twisted approximately 45° relative to one another and the eight aryl groups are arranged in a propeller orientation.

$[2,5\text{-Ph}_2\text{-3,4-Tol}_2(\eta^4\text{-C}_4\text{CO})]\text{Ru}_2(\text{CO})_2$ (**7**). Prolonged heating of $\text{Ru}_3(\text{CO})_{12}$ and cyclopentadienone **4** in heptane for 48 h led to the precipitation of ruthenium dimer **7** as a mustard yellow powder in 74% yield (Scheme 6).¹⁴ The tolyl methyl ^1H NMR resonances made it easy to distinguish dimer **7** ($\delta 1.69$) from diruthenium hydride complex **6** ($\delta 1.79$). The X-ray crystal structure of **7** (see Supporting Information) confirmed its dimeric structure.¹⁵

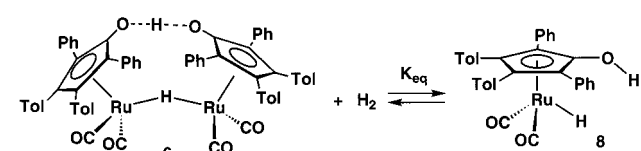
$[2,5\text{-Ph}_2\text{-3,4-Tol}_2(\eta^5\text{-C}_4\text{COH})\text{Ru}(\text{CO})_2\text{H}]$ (**8**). Reaction of either H_2 or formic acid with diruthenium complex **6** in $\text{THF-}d_8$ produced the monomeric hydroxycyclopentadienyl ruthenium hydride **8** (Scheme 7). A resealable NMR tube containing a solution of **6** in $\text{THF-}d_8$ under 1 atm of H_2 at -78°C was sealed and heated at 80°C . After 2 h, the hydride resonance for **6** at $\delta -18.23$ had decreased in intensity and a new hydride resonance assigned to **8** appeared at $\delta -9.76$. The 1:2 ratio of these resonances indicated 50% of **6** had been converted to **8**. After 8 h, equilibrium was reached and a 98:2 mixture of **8**:**6** was observed ($K_{\text{eq}} = [\mathbf{8}]^2/[\mathbf{6}][\text{H}_2] \approx 1 \text{ atm}^{-1}$).

(13) In contrast, $(\eta^4\text{-C}_4\text{Ph}_4\text{CO})\text{Ru}(\text{CO})_3$ exhibits η^4 -coordination with a $\text{Ru}(1)\text{-C}(1)$ bond distance of 2.53 \AA and a $\text{C}(1)\text{-O}(1)$ bond length of 1.22 \AA . Blum, Y.; Shvo, Y.; Chodos, D. F. *Inorg. Chim. Acta* **1985**, *97*, L25.

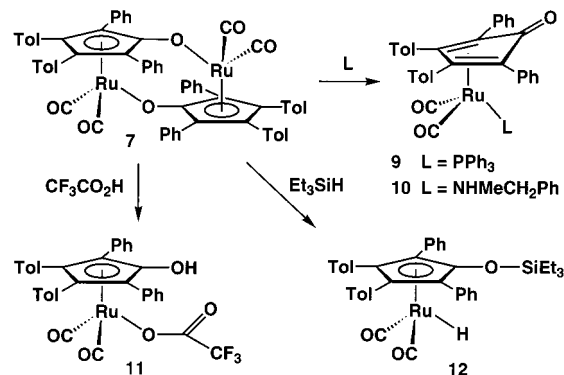
(14) **7** was identified by comparing its spectroscopic data to that of analogous complexes. Mays, M. J.; Morris, M. J.; Raithby, P. R.; Shvo, Y.; Czarkie, D. *Organometallics* **1989**, *8*, 1162.

(15) The structure of **7** is similar to that obtained for the tetraphenyl analogue by Shvo and Mays.¹⁴ They described the dimer as having η^4 -cyclopentadienyl ligands with ketonic carbonyls bound to the second Ru. However, we believe that both compounds are better described as having the η^5 -cyclopentadienyl rings with alkoxy oxygens bound to the second ruthenium. The 2.40 \AA $\text{Ru}(1)\text{-C}(1)$ and the 1.28 \AA $\text{C}(1)\text{-O}(1)$ bond lengths of **7** are very similar to the related bond lengths in diruthenium hydroxycyclopentadienyl ruthenium hydride **6** and support the formulation of **7** as an η^5 -alkoxycyclopentadienyl complex.

Scheme 7



Scheme 8



The ^1H and ^{13}C NMR spectra of **8** were consistent with its formulation as a hydroxycyclopentadienyl ruthenium hydride. In the ^1H NMR spectrum, a hydride resonance was observed at $\delta -9.76$ and a broad singlet assigned to the hydroxyl proton was observed at $\delta 8.60$. A single tolyl methyl resonance was observed at $\delta 2.17$, indicating **8** had formed without any byproducts. In the ^{13}C NMR spectrum of **8**, the cyclopentadienyl C–O resonance appeared at $\delta 137$ and the RuCO resonance appeared $\delta 203$.¹⁶

The equilibrium constant for formation of **8** from H_2 was much less favorable in hydrocarbon solvents than in THF. Essentially complete conversion to **8** was achieved under only 1 atm of H_2 in $\text{THF-}d_8$. However, when **6** was heated under 1 atm of H_2 at 80°C in C_6D_6 , incomplete conversion to **8** was seen and a 75:25 equilibrium mixture of **6**:**8** was formed after 72 h ($K_{\text{eq}} = [\mathbf{8}]^2/[\mathbf{6}][\text{H}_2] \approx 0.02 \text{ atm}^{-1}$).¹⁷ Solutions of **8** in toluene- d_8 , CD_3CN , and $\text{DMSO-}d_6$ were conveniently prepared from THF solutions of **8** by removing THF under high vacuum and dissolving the resulting oily solid in the solvent of choice.¹⁸

The reaction of diruthenium hydride **6** with HCO_2H produced solutions of **8** containing excess formic acid. When a 10-fold excess of 96% HCO_2H was added to a $\text{THF-}d_8$ solution of **6**, no reaction was observed at room temperature. However, upon heating at 80°C , vigorous evolution of gas occurred. After 10 min, the evolution of gas had ceased and ^1H NMR showed that **6** had been completely converted to **8**.

$[2,5\text{-Ph}_2\text{-3,4-Tol}_2(\eta^4\text{-C}_4\text{CO})]\text{Ru}(\text{CO})_2\text{PPh}_3$ (**9**) and $[2,5\text{-Ph}_2\text{-3,4-Tol}_2(\eta^4\text{-C}_4\text{CO})]\text{Ru}(\text{CO})_2\text{NH}(\text{CH}_3)(\text{CH}_2\text{Ph})$ (**10**) were synthesized by ligand addition to ruthenium dimer **7** at room temperature (Scheme 8). Addition of PPh_3 to a CH_2Cl_2 solution of **7** led to the isolation of phosphine adduct **9** as a pale yellow powder in 74% yield.¹⁹ Similarly, addition of $\text{NH}(\text{CH}_3)(\text{CH}_2\text{Ph})$ to a CH_2Cl_2 solution of **7** gave a 79% yield of amine adduct **10** as a dark green solid.²⁰

$[2,5\text{-Ph}_2\text{-3,4-Tol}_2(\eta^5\text{-C}_4\text{COH})\text{Ru}(\text{CO})_2(\text{O}_2\text{CCF}_3)]$ (**11**). Addition of excess $\text{CF}_3\text{CO}_2\text{H}$ to a CH_2Cl_2 solution of ruthenium

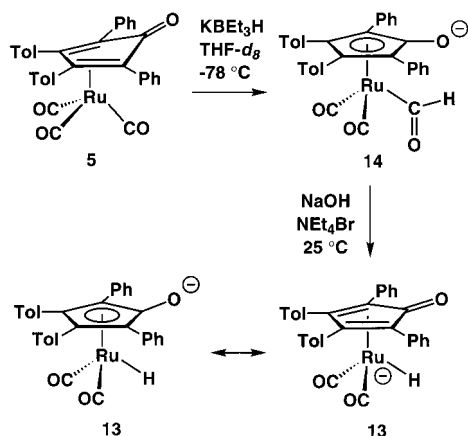
(16) The spectroscopic data closely match the reported data for the tetraphenyl analogue.⁶

(17) Shvo and Mays attributed the thermodynamic stability of **2** in THF to intermolecular hydrogen bonding between the hydroxy group and THF, which prevents loss of H_2 and reversion to **3**.¹⁴

(18) Solutions prepared this way contained 0.5–1.0 equiv of THF/Ru .

(19) A crystal structure of the tetraphenyl analogue was recently published. Yamazaki, S.; Taira, Z. *J. Organomet. Chem.* **1999**, *578*, 61.

Scheme 9



dimer **7** followed by addition of pentane led to the isolation of the hydroxycyclopentadienyl trifluoroacetate complex **11** as a light green powder in 85% yield (Scheme 8). The structure of **11** was confirmed by X-ray crystallography (see Supporting Information).

$[\text{2,5-Ph}_2\text{-3,4-Tol}_2(\eta^5\text{-C}_4\text{COSiEt}_3)\text{Ru}(\text{CO})_2\text{H}]$ (**12**) was prepared by addition of SiEt_3H to a CH_2Cl_2 solution of ruthenium dimer **7** (Scheme 8). The formation of **12** can be rationalized as an oxidative addition of Et_3SiH to a monomeric cyclopentadienone ruthenium dicarbonyl intermediate. The ^1H NMR spectrum (C_6D_6) showed a single tolyl CH_3 resonance at δ 1.81 and a hydride resonance at δ -9.20.

$\text{NEt}_4^+[\text{2,5-Ph}_2\text{-3,4-Tol}_2(\eta^4\text{-C}_4\text{CO})\text{Ru}(\text{CO})_2\text{H}]^-$ (**13**). The anionic alkoxy-cyclopentadienyl hydride **13** was synthesized to compare its reactivity toward aldehydes with that of the hydroxycyclopentadienyl hydride **8**. The most convenient preparative route to pure **13** was addition of a THF solution of KBEt_3H to a suspension of NEt_4Br and **5** in THF at $-78\text{ }^\circ\text{C}$ (Scheme 9). After the mixture was warmed to room temperature for 20 min and aqueous NaOH workup to destroy excess borohydride, **13** was isolated in 77% yield as an off-white powder. The ^1H NMR spectrum of **13** exhibited a hydride resonance at δ -9.68 and a single tolyl methyl resonance at δ 2.15.

The intermediacy of formyl complex **14** in the synthesis of **13** was demonstrated by ^1H NMR spectroscopy (Scheme 9). After addition of KBEt_3H to a $\text{THF-}d_8$ solution of tricarbonyl **5** at $-78\text{ }^\circ\text{C}$ and warming to $-30\text{ }^\circ\text{C}$, the ^1H NMR spectrum of the golden yellow solution exhibited a single tolyl methyl resonance at δ 2.17 and a singlet at δ 12.70 characteristic of a metal formyl group.²¹ Formyl complex **14** underwent decarbonylation to $\text{K}^+[\text{2,5-Ph}_2\text{-3,4-Tol}_2(\eta^5\text{-C}_4\text{CO})\text{Ru}(\text{CO})_2\text{H}]^-$ with $t_{1/2} = 15\text{ min}$ at $23\text{ }^\circ\text{C}$.

The X-ray crystal structure of **13** (Figure 2) supports η^4 -coordination of the cyclopentadienone ligand to the Ru center. The long $\text{Ru}(1)\text{-C}(1)$ distance of 2.45 Å, the short $\text{C}(1)\text{-O}(1)$ bond length of 1.244 Å, and the 12.7° tilt of the $\text{C}(1)\text{-O}(1)$ bond out of the plane defined by $\text{C}(2)\text{-C}(5)$ provide evidence for η^4 -coordination.

Stability of Hydroxycyclopentadienyl Ruthenium Hydride 8. Solutions of hydroxycyclopentadienyl ruthenium hydride **8** were stable under H_2 , but decomposed under N_2 or in the presence of air. In $\text{THF-}d_8$ under N_2 at room temperature, the rate of reversion to the diruthenium complex **6** and H_2 was slow ($t_{1/2} \approx 1\text{--}2\text{ days}$).

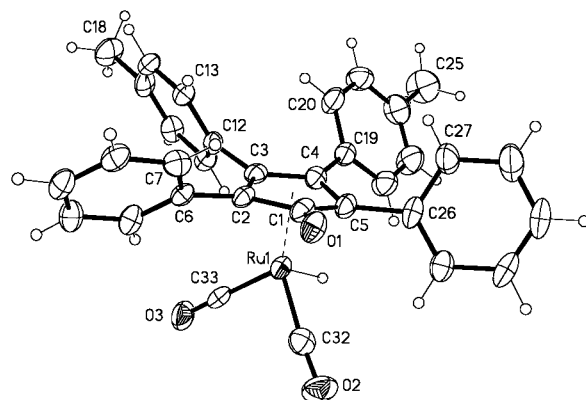
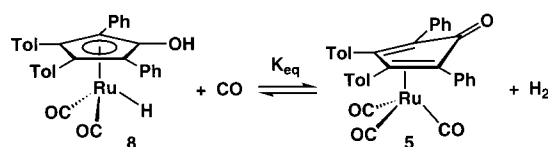
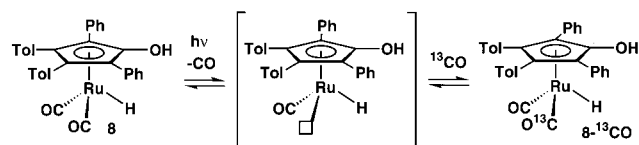


Figure 2. X-ray Crystal Structure of $\text{NEt}_4^+[\text{2,5-Ph}_2\text{-3,4-Tol}_2(\eta^4\text{-C}_4\text{CO})\text{Ru}(\text{CO})_2\text{H}]^-$ (**13**). Thermal ellipsoids are drawn at 50% probability. The NEt_4^+ cation is omitted for clarity.

Scheme 10



Scheme 11



When a solution of **8** in $\text{THF-}d_8$ was heated at $80\text{ }^\circ\text{C}$ under 1.7 atm CO , an equilibrium between **8** and dienone ruthenium tricarbonyl complex **5** was slowly established (Scheme 10). After 72 h, an equilibrium 87:13 mixture of **5** (δ 2.21):²² **8** (δ 2.16) was observed ($K_{\text{eq}} = [\text{5} = 0.0226\text{ mmol}]/[\text{H}_2 = 0.0226\text{ mmol}]/[\text{8} = 0.0034\text{ mmol}][\text{CO} = 0.1\text{ mmol}] = 1.5$). The equilibrium was also approached from the opposite direction. When a solution of **5** in $\text{THF-}d_8$ was heated at $80\text{ }^\circ\text{C}$ under 1.7 atm of H_2 for 72 h, a 30:70 equilibrium mixture of **5** and **8** was established ($K_{\text{eq}} = [\text{5} = 0.0057\text{ mmol}][\text{H}_2 = 0.1\text{ mmol}]/[\text{8} = 0.0133\text{ mmol}][\text{CO} = 0.0133\text{ mmol}] = 3.2$). In both experiments the formation of diruthenium complex **6** was not detected.

Exchange of ^{13}CO with hydroxycyclopentadienyl ruthenium hydride **8** was studied to determine whether reversible CO dissociation occurs. Fluorescent room light was found to promote ^{13}CO exchange. A $\text{THF-}d_8$ solution of **8** under 1.5 atm of ^{13}CO exposed to room light was monitored by ^1H NMR spectroscopy. After 15 min, a three-line pattern was observed at δ -9.76 consisting of a center line for unlabeled **8** flanked by a doublet ($^2J_{\text{CH}} = 9.5\text{ Hz}$) for monolabeled $\text{8-}^{13}\text{CO}$ (4:1 = $\text{8:8-}^{13}\text{CO}$) (Scheme 11). After 1.5 h in room light, a five-line pattern was observed due to the superposition of a central line for unlabeled **8**, a doublet for $\text{8-}^{13}\text{CO}$, and a triplet ($^2J_{\text{CH}} = 9.5\text{ Hz}$) for double-labeled $\text{8-(}^{13}\text{CO)}_2$ (1:1:0.2 = $\text{8:8-}^{13}\text{CO}:\text{8-(}^{13}\text{CO)}_2$). The ^{13}CO exchange rate was slowed dramatically when the experiment was repeated in an NMR tube kept in the dark. After 1 h, less than 5% ^{13}CO incorporation was seen. The observation of facile CO exchange at room temperature requires

(21) Gladysz, J. A. *Adv. Organomet. Chem.* **1982**, *20*, 1.

(22) The reaction was stopped at that point, and the $\text{THF-}d_8$ was removed in vacuo and replaced with C_6D_6 . The ^1H NMR spectrum in C_6D_6 confirmed that the resonance at δ 2.21 in $\text{THF-}d_8$ corresponded to a resonance at δ 1.82 in C_6D_6 , the tolyl resonance for tricarbonyl **5**.

(20) Similar amine complexes have been synthesized. (a) Abed, M.; Goldberg, I.; Stein, Z.; Shvo, Y. *Organometallics* **1988**, *7*, 2054. (b) Shvo, Y.; Abed, M.; Laine, Blum, Y.; Laine, R. M. *Isr. J. Chem.* **1986**, *27*, 267.

serious consideration of photochemically induced CO dissociation as a possible step in reactions of **8**.

Acidity of Hydroxyl Proton in Hydroxycyclopentadienyl Hydride 8. Knowledge of the acidity²³ of the hydroxy proton of **8** is crucial in evaluating the role of proton transfer in the reduction of PhCHO by **8**. CH₃CN was chosen as the solvent for determination of the pK_a of **8** because it allows comparison with a broad spectrum of organic acids.²⁴ Norton's IR method for determination of the pK_a of metal carbonyl hydrides in CH₃CN was readily adapted to the study of **8**.²⁵

When NEt₃ (0.072 M, pK_a = 18.5 in CH₃CN) was added to a 0.070 M CH₃CN solution of **8**, IR bands due to **8** at 2014 and 1954 cm⁻¹ decreased in intensity and new bands at 1985 and 1920 cm⁻¹ assigned to NEt₃H⁺[2,5-Ph₂-3,4-Tol₂(η⁵-C₄CO)Ru(CO)₂H]⁻ (**15**) grew in. A 1:3.6 ratio of **8**:**15** was determined by comparing the absorbances with independently obtained molar extinction coefficients. The pK_a of **8** was calculated to be 17.5.²⁶ When 1 equiv of pyridine (pK_a = 12.4 in CH₃CN) was added to a CH₃CN solution of **8**, no deprotonation was observed. When 1 equiv of 1,1,3,3-tetramethylguanidine (pK_a = 23.3 in CH₃CN) was added to a CH₃CN solution of **8**, complete deprotonation to the guanidinium salt was observed.

The hydroxyl proton of **8** in CH₃CN is 9 pK_a units more acidic than phenol (pK_a = 26.6 in CH₃CN) and 3 pK_a units more acidic than benzoic acid (pK_a = 20.7 in CH₃CN).²⁷ The moderately strong acidity of the hydroxyl proton must be considered as an important factor in the reaction of **8** with PhCHO.

Kinetics of PhCHO Reduction by Hydroxycyclopentadienyl Ruthenium Hydride 8. When an excess of PhCHO was added to a THF-*d*₈ solution of **8** at -78 °C and then warmed to room temperature, complete disappearance of the hydride resonance at δ -9.76 and the hydroxyl resonance at δ 8.60 was observed in the ¹H NMR spectrum within 10 min. New resonances were observed at δ 4.57 corresponding to the CH₂ group of PhCH₂OH, and at δ -18.23 for the diruthenium hydride **6** (Scheme 12). The NMR yield of PhCH₂OH was determined with ferrocene as an internal standard. The formation of PhCH₂OH was independently confirmed by gas chromatography.

The kinetics of PhCHO reduction by **8** were measured by adding an excess (typically >10-fold excess) of aldehyde to a THF-*d*₈ solution of **8** at -78 °C and monitoring the disappearance of **8** by ¹H NMR spectroscopy in an NMR probe cooled to -10 °C. The disappearance of **8** followed pseudo-first-order kinetics to over 80% conversion, indicating a first-order dependence on **8**. Four kinetic runs were carried out at -10 °C with aldehyde concentrations of 0.8 (*k*_{obs} = 5.0 × 10⁻⁴ s⁻¹), 1.0 (*k*_{obs} = 6.2 × 10⁻⁴ s⁻¹), 1.2 (*k*_{obs} = 8.0 × 10⁻⁴ s⁻¹), and 1.6 M (*k*_{obs} = 1.0 × 10⁻³ s⁻¹). A linear plot of *k*_{obs} vs PhCHO concentration established a first-order dependence on PhCHO.

(23) The few pK_a values determined for hydroxycyclopentadienyl ligands in water are in the same range as organic acids. [C₅H₄OH]Fe(CO)₂Cl was calculated to have a pK_a of ~4 in H₂O. Weiss, E.; Merényi, R.; Hübel, W. *Chem. Ber.* **1962**, *95*, 1170.

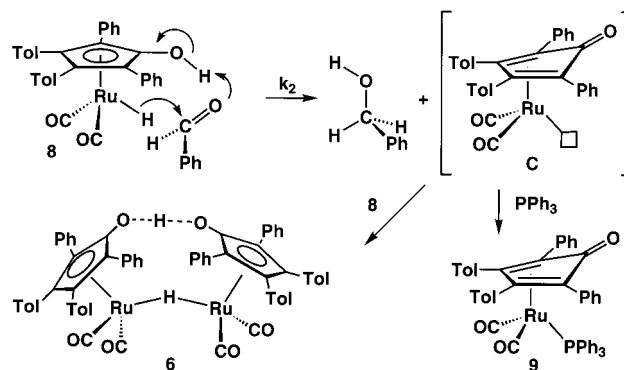
(24) pK_a measurements are available for a much narrower range of compounds in THF. Coetzee, J. F. *Prog. Phys. Org. Chem.* **1967**, *4*, 45.

(25) (a) Jordan, R. F.; Norton, J. R. *J. Am. Chem. Soc.* **1982**, *104*, 1255. (b) Moore, E. J.; Sullivan, J. M.; Norton, J. R. *J. Am. Chem. Soc.* **1986**, *108*, 2257.

(26) *K*_{eq} = [NEt₃H⁺][**15**]/[NEt₃][**8**]; pK_a(**8**-OH) = pK_a(NEt₃H⁺) + p*K*_{eq}.

(27) In general, the pK_a values of organic -OH acids in CH₃CN are higher relative to ammonium ions than in water because CH₃CN solvates ionic species poorly, and deprotonation of the cationic ammonium salts to neutral amines is thermodynamically favored in CH₃CN. (a) Chantooni, M. K., Jr.; Kolthoff, I. M. *J. Am. Chem. Soc.* **1970**, *92*, 7025. (b) Kolthoff, I. M.; Chantooni, M. K., Jr.; Bhowik, S. *J. Am. Chem. Soc.* **1966**, *88*, 5430. For a recent illustrative example see: Shafiq, F.; Szalda, D. J.; Creutz, C.; Bullock R. M. *Organometallics* **2000**, *19*, 824.

Scheme 12



Equation 1 shows the second rate law for PhCHO reduction. The second-order rate constant at -10 °C is *k*₂ = (3.0 ± 0.2) × 10⁻⁴ M⁻¹ s⁻¹.²⁸

$$-\frac{d[\mathbf{8}]}{dt} = -2 \frac{d[\text{PhCHO}]}{dt} = 2 \frac{d[\text{PhCH}_2\text{OH}]}{dt} = 2 \frac{d[\mathbf{6}]}{dt} = 2k_2[\mathbf{8}][\text{PhCHO}] \quad (1)$$

The temperature dependence of the rate of reduction of PhCHO by **8** was measured between 0 and -15 °C: *k*₂ = (7.7 ± 0.5) × 10⁻⁴ M⁻¹ s⁻¹ at 0 °C, (5.9 ± 0.4) × 10⁻⁴ M⁻¹ s⁻¹ at -5 °C, and (2.0 ± 0.3) × 10⁻⁴ M⁻¹ s⁻¹ at -15 °C. An Eyring plot gave Δ*H*[‡] = 12.0 ± 1.5 kcal mol⁻¹ and Δ*S*[‡] = -28 ± 5 eu. The high negative entropy of activation is consistent with an associative reaction in which the transition state for hydrogen transfer is highly ordered.

The rate of PhCHO reduction was not inhibited by CO pressure. Essentially the same rate of hydride disappearance was observed under N₂ as under 1 atm of CO at 0 °C (*k*_{obs} = 1.13 × 10⁻³ s⁻¹).²⁹ This is consistent with the fact that PhCHO reduction is faster than ¹³CO exchange in the dark.

Trapping of Dienone Dicarbonyl Ruthenium Intermediate C. The stoichiometry and reaction products suggest that hydrogen transfer from **8** to PhCHO initially produces a coordinatively unsaturated dienone ruthenium dicarbonyl intermediate **C** that is trapped by an additional equivalent of **8** to give the diruthenium hydride **6**. In an effort to intercept intermediate **C**, the reaction of **8** with PhCHO (1.0 M) was carried out at 0 °C in the presence of PPh₃ (0.4 M).³⁰ In addition to the disappearance of **8** and the formation of PhCH₂OH, a new tolyl resonance at δ 2.17 in the ¹H NMR spectrum and a new phosphorus resonance at δ 38.4 in the ³¹P NMR spectrum provided evidence for the formation of [2,5-Ph₂-3,4-Tol₂(η⁴-C₄CO)]Ru(CO)₂PPh₃ (**9**). The absence of a bridging hydride resonance in the ¹H NMR spectrum showed that none of the diruthenium hydride **6** was formed in the reaction. Thus, 0.4 M

(28) Under catalytic conditions, carbonyl reduction by **8** is reversible. Reduction of PhCDO (1.0 M) by **8** at 0 °C resulted in no D incorporation into the product **6**. This result illustrates that under the stoichiometric conditions used in these kinetic studies, no reversible alcohol dehydrogenation occurs.

(29) The slightly slower observed rate for hydride disappearance is attributable to the trapping of approximately 20% of dienone dicarbonyl intermediate **C** by CO to form tricarbonyl **5**.

(30) A control experiment showed that **8** does not react with PPh₃ at room temperature. This is somewhat surprising since ¹³CO exchange occurs into **8** under these conditions. This result may be accounted for by the steric bulk of the tetraarylcyclopentadienyl ligand. For a similar example, see: Adams, H.; Bailey, N. A.; Browning, A. F.; Ramsden, J. A.; White, C. J. *Organomet. Chem.* **1990**, *387*, 305.

Table 1. Kinetic Deuterium Isotope Effects on the Reduction of PhCHO by **8**

$k_{\text{OHRuH}}/k_{\text{OHRuD}}$	1.5 ± 0.2
$k_{\text{OHRuH}}/k_{\text{ODRuH}}$	2.2 ± 0.1
$k_{\text{OHRuH}}/k_{\text{ODRuD}}$	3.6 ± 0.3
$k_{\text{ODRuH}}/k_{\text{ODRuD}}$	1.6 ± 0.2
$k_{\text{OHRuD}}/k_{\text{ODRuD}}$	2.3 ± 0.4

PPh₃ is a much more efficient trap for the intermediate **C** than is the ruthenium hydride **8**.

The rate of conversion of PhCHO to PhCH₂OH was the same as in the absence of PPh₃. However, because only 1 equiv of **8** was consumed in the presence of PPh₃ compared with 2 equiv in the absence of PPh₃, the rate of disappearance of **8** is only half as rapid in the presence of PPh₃ (eq 2). The second-order rate constant in the presence of PPh₃ ($k_2 = (9.1 \pm 0.5) \times 10^{-4} \text{ M}^{-1} \text{ s}^{-1}$ at 0 °C) was approximately the same as in the absence of PPh₃ ($k_2 = (7.7 \pm 0.6) \times 10^{-4} \text{ M}^{-1} \text{ s}^{-1}$ at 0 °C).

$$-\frac{d[\mathbf{8}]}{dt} = -\frac{d[\text{PhCHO}]}{dt} = \frac{d[\text{PhCH}_2\text{OH}]}{dt} = \frac{d[\mathbf{9}]}{dt} = k_2[\mathbf{8}][\text{PhCHO}] \quad (2)$$

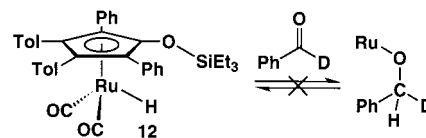
Deuterium Isotope Effects. Isotope effects on PhCHO reduction were investigated by selective deuteration of the hydroxy and hydride positions of **8**. To ensure that adventitious proton sources (small amounts of PhCOOH or H₂O) did not attenuate the kinetic isotope effect on the -OH proton, D₂O was added to the reactions.³¹ As a control, the rate of PhCHO (1.0 M) reduction at 0 °C was measured in the presence of H₂O (0.2 M). The reaction proceeded with $k_{\text{obs}} = (1.60 \pm 0.02) \times 10^{-3} \text{ s}^{-1}$, a small increase from the rate in the absence of water. The rate of PhCHO (1.0 M) reduction at 0 °C in the presence of D₂O (0.2 M) proceeded with $k_{\text{obs}} = (7.3 \pm 0.1) \times 10^{-4} \text{ s}^{-1}$. Dideuterated **8-d₂** (>90% isotopic purity at the hydride position)³² was prepared by heating a THF-*d*₈ solution of **7** under D₂ (1 atm at -196 °C) at 80 °C for 8 h. PhCHO (1.0 M) reduction by **8-d₂** at 0 °C in the presence of H₂O (0.2 M) proceeded with $k_{\text{obs}} = (1.04 \pm 0.10) \times 10^{-3} \text{ s}^{-1}$. PhCHO (1.0 M) reduction by **8-d₂** in the presence of D₂O (0.2 M) proceeded with $k_{\text{obs}} = (4.5 \pm 0.3) \times 10^{-4} \text{ s}^{-1}$. The deuterium isotope effects determined from these rates are summarized in Table 1.

PhCHO Reduction in the Presence of CF₃CO₂H. The mechanism shown in Scheme 12 involves simultaneous transfer of hydride from ruthenium and protonation of the PhCHO oxygen by the hydroxy group. This proton transfer takes advantage of the high acidity of the hydroxycyclopentadienyl group. To test whether other Bronsted acids could act as general acids to transfer a proton to the benzaldehyde oxygen and accelerate hydride transfer from **8**, the rate of reaction of **8** with PhCHO (1.0 M) in the presence of CF₃CO₂H (0.4 M, p*K*_a = 12.6 in CH₃CN)³³ at 0 °C was measured by ¹H NMR spectroscopy ($k_2 = (1.09 \pm 0.03) \times 10^{-3} \text{ M}^{-1} \text{ s}^{-1}$). The hydride resonance of **8** disappeared and new resonances for PhCH₂OH

(31) In the absence of added D₂O, nonreproducible and internally inconsistent results were obtained for kinetic isotope effects on the hydroxyl proton.

(32) At room temperature the OH proton of **8** readily exchanged with external D₂O in THF-*d*₈, but no exchange with Ru-H was observed. When a THF-*d*₈ solution of **8** and D₂O was heated at 80 °C exchange with Ru-H was observed. This exchange was faster than exchange of **8** with D₂ in THF-*d*₈. These results suggest that **8** is in equilibrium with a dihydrogen complex that dissociates H₂, leading to exchange with D₂. Casey, C. P.; Singer, S. W. Unpublished results.

(33) Jasinski, T.; El-Harakany, A. A.; Halaka, F. G.; Sadek, H. *Croat. Chem. Acta* **1978**, *51*, 1.

Scheme 13

and a new tolyl resonance at δ 2.18 assigned to hydroxy-trifluoroacetate complex **11** appeared. No resonances corresponding to the diruthenium hydride **6** were observed. Apparently the initially formed intermediate **C** is trapped by oxidative addition of trifluoroacetic acid.

Even though CF₃CO₂H is a much stronger acid than the hydroxy group of **8**, the rate of PhCHO reduction by **8** in the presence of 0.4 M CF₃CO₂H was less than twice as fast as in the absence of acid. This indicates that the hydroxyl group of **8** is an unusually effective intramolecular general acid for promotion of hydride transfer from ruthenium to PhCHO.

Reduction of PhCHO by the Anionic Alkoxy-cyclopentadienyl Ruthenium Hydride 13. The relative importance of the hydride donor strength of the ruthenium hydride and the acidity of the hydroxycyclopentadienyl in PhCHO reduction was investigated by studying the reaction of the anionic alkoxy-cyclopentadienyl ruthenium hydride NEt₄⁺[2,5-Ph₂-3,4-Tol₂(η^5 -C₄CO)Ru(CO)₂H]⁻ (**13**) with PhCHO. This complex should be a better hydride donor than **8** because of the negative charge on the complex, but it does not possess an acidic proton. No reaction between PhCHO (1.0 M) and hydride anion **13** in CD₃-CN was observed after 80 min at room temperature. The purity of the PhCHO used in the reduction altered the rate of hydride disappearance markedly. While no reduction of freshly distilled PhCHO was observed, relatively fast reductions were observed with undistilled PhCHO stored in air ($t_{1/2} \approx 15$ min at room temperature for a 1.0 M solution).³⁴ Addition of the aldehyde oxidation product PhCO₂H speeded up reduction rates dramatically.³⁵ The accelerating effect of PhCO₂H in the reductions with anionic hydride **13** underscores the critical importance of the general acid catalysis in the reductions with hydroxy-hydride **8**.

No PhCHO Reduction by Triethylsilyloxycyclopentadienyl Ruthenium Hydride 12. To further explore the role of the hydroxycyclopentadienyl proton in mediating the reduction of PhCHO, the reaction of PhCHO with [2,5-Ph₂-3,4-Tol₂(η^5 -C₄CO)SiEt₃Ru(CO)₂H] (**12**), which has no acidic hydrogen, was studied. No reaction between PhCHO and the triethylsilyloxy-hydride **12** in C₆D₆ was observed after 24 h at room temperature.³⁶ This result confirms the importance of the hydroxyl in promoting the carbonyl reduction. To test for the possibility that hydride transfer might occur reversibly from **12** to PhCHO to generate a benzyl alkoxide intermediate, a solution of **12** and PhCDO in C₆D₆ was monitored after 24 h at room temperature. No decrease in the hydride resonance of **12** at δ -9.20 was seen, indicating that no reversible hydride addition to **12** was occurring (Scheme 13).

Reduction of Other Polar Double Bonds by 8. Reduction of PhCOMe by **8** occurred more slowly than reduction of PhCHO. Reaction of **8** with PhCOMe (1.2 M) in THF-*d*₈ at 22 °C gave 1-phenylethanol and diruthenium complex **6**. The rate

(34) In contrast, the rate of PhCHO reduction by **8** was the same with pure or PhCOOH-contaminated PhCHO.

(35) The requirement of an acid to promote carbonyl reduction by anionic transition metal hydrides has been previously observed. Gaus, P. L.; Kao, S. C.; Youngdahl, K.; Darenbourg, M. Y. *J. Am. Chem. Soc.* **1985**, *107*, 2428.

(36) Reactions with **12** were done in C₆D₆ because the complex was very sensitive to hydrolysis in THF-*d*₈.

constant for reduction was $k_2 = (2.0 \pm 0.2) \times 10^{-4} \text{ M}^{-1} \text{ s}^{-1}$ at 22 °C. Extrapolating the rate of reduction of PhCHO to 22 °C ($k = 6.0 \times 10^{-3} \text{ M}^{-1} \text{ s}^{-1}$) indicates that PhCOME reduction is 30 times slower than PhCHO reduction.³⁷

The facile hydrogen transfer to carbonyl groups led us to examine reduction of imines. From Shvo's work, we anticipated that the resulting amine after hydrogen transfer would bind to the dienone dicarbonyl intermediate **C** to form a stable amine adduct **10**. Measurement of the rate of hydrogen transfer to MeN=CHPh was attempted at -10 °C to compare directly with the rate of PhCHO reduction, but the reaction proceeded too quickly to accurately measure a rate. At -25 °C, the rate constant for imine reduction was $k_2 = (2.63 \pm 0.05) \times 10^{-3} \text{ M}^{-1} \text{ s}^{-1}$. Extrapolating the rate of PhCHO reduction to -25 °C ($k = 1.0 \times 10^{-4} \text{ M}^{-1} \text{ s}^{-1}$) indicates that imine reduction is 26 times faster than PhCHO reduction. The product of the reaction is amine adduct **10**, which was confirmed by independent synthesis.

Solvent Effects on Hydrogen Transfer. The rate of hydrogen transfer from hydroxy-hydride **8** to PhCHO was significantly increased by changing the solvent from THF-*d*₈ to toluene-*d*₈. The kinetics of the reaction of **8** with PhCHO (1.0 M) in toluene-*d*₈ at -45 °C were monitored by following the disappearance of the hydride resonance of **8** ($k_{\text{obs}} = 1.2 \times 10^{-3} \text{ s}^{-1}$, $k_2 = (6.0 \pm 0.2) \times 10^{-4} \text{ M}^{-1} \text{ s}^{-1}$, $\Delta G^\ddagger = 16.6 \text{ kcal mol}^{-1}$). The rate of hydrogen transfer to PhCHO was approximately 50 times faster in toluene than THF ($\Delta\Delta G^\ddagger = 1.8 \text{ kcal mol}^{-1}$). Hydrogen transfer to PhCOCH₃ ($k_2 = (2.3 \pm 0.2) \times 10^{-4} \text{ M}^{-1} \text{ s}^{-1}$ at -10 °C) and MeN=CHPh ($k_2 = (4.50 \pm 0.25) \times 10^{-3} \text{ M}^{-1} \text{ s}^{-1}$ at -60 °C) was also faster in toluene than THF.³⁸

Alkene Reactivity. While hydrogen transfer from **8** to polar double bonds occurs rapidly below room temperature, cyclohexene was unreactive. No reaction was observed at room temperature when an excess of cyclohexene was added to a THF-*d*₈ solution of **8**. At 80 °C, loss of H₂ from **8** to form diruthenium complex **6** occurred without observable hydrogenation of cyclohexene. However, when **8** and cyclohexene were heated at 80 °C under H₂ (1 atm), slow catalytic hydrogenation of cyclohexene occurred (~5 turnovers in 24 h).³⁹ Similar turnover rates were observed when a toluene-*d*₈ solution of triethylsiloxy-hydride **12** and excess cyclohexene was heated at 80 °C under H₂. Under the conditions of this catalytic hydrogenation, hydrides **8** and **12** were the only observable Ru species.⁴⁰

Discussion

Concerted Hydrogen Transfer Mechanism. We have obtained persuasive evidence that reduction of aldehydes by **8** occurs by simultaneous transfer of hydride from ruthenium and of a proton from the CpOH group (Scheme 12). During the

(37) Using activation parameters obtained from PhCHO reductions corresponds to a difference in activation barriers of 2.0 kcal mol⁻¹ (22.3 kcal mol⁻¹ vs 20.3 kcal mol⁻¹).

(38) PhCHO reductions were also run in CD₃CN ($k = (9.7 \pm 0.6) \times 10^{-3} \text{ M}^{-1} \text{ s}^{-1}$ at 0 °C) and in DMSO-*d*₆ ($k = (1.00 \pm 0.04) \times 10^{-3} \text{ M}^{-1} \text{ s}^{-1}$ at 21 °C). These measured rates indicate that the strength of hydrogen bonding interactions between the hydroxyl proton of **8** and the solvent dramatically changes the rate of aldehyde reduction.

(39) No catalytic hydrogenation was observed when **8** and excess HCO₂H were heated to 80 °C in the presence of cyclohexene in THF-*d*₈.

(40) At room temperature, **8** catalyzes the isomerization of 1-pentene to a thermodynamic mixture of *cis*- and *trans*-2-pentene. Addition of methyl acrylate to **8** forms an alkyl complex by *cis* hydride addition across the C=C double bond. These alkene reactions are promoted by light, so photochemical CO dissociation appears to be the first step in these reactions. It is unclear whether photochemical CO dissociation is involved in catalytic hydrogenation of alkenes at elevated temperature. Casey, C. P.; Singer, S. W. Unpublished results.

hydrogen transfer, the aldehyde is outside the coordination sphere of the metal. The second-order rate law requires a transition state involving both **8** and the aldehyde; the large negative $\Delta S^\ddagger = -28 \text{ eu}$ is consistent with a concerted mechanism.

The observation of primary deuterium isotope effects for both Ru-D and O-D provides the strongest evidence for a concerted hydrogen transfer mechanism involving both Ru-H and O-H bond breaking in the transition state. Ru-H transfer from one molecule of **8** concerted with O-H transfer from a *second* molecule of **8** can be excluded since such a mechanism would require a rate dependence on [**8**]². The kinetic isotope effect of 1.5 ± 0.2 for Ru-D is similar to previously measured isotope effects for rate-determining hydride additions.⁴¹ The isotope effect of 2.2 ± 0.1 for O-D is consistent with rate-determining proton transfer, though it is smaller than the isotope effect reported for proton transfer in many acid-catalyzed reactions.⁴² As expected for a concerted reaction, the product of the two individual isotope effects ($1.5 \times 2.2 = 3.3$) is within experimental error of the combined D isotope effect measured for RuD-OD (3.6 ± 0.3).

Unfortunately, there are no experimental or theoretical studies of kinetic isotope effects on concerted proton and hydride transfer in organometallic complexes to compare to the isotope effects observed here.⁴³ However, a concerted hydrogen transfer mechanism has been proposed for certain dehydrogenase enzymes.⁴⁴ In particular, theoretical studies on models of lactate dehydrogenase, which catalyzes the redox interconversion of lactate and pyruvate, have estimated isotope effects for a concerted proton and hydride transfer.⁴⁵ Calculated primary kinetic isotope effects for a dihydropyridine/formaldehyde/imidazolium system were 1.6–2.0 for hydride transfer and 2.3–2.4 for proton transfer.⁴⁶ Isotope effects of similar magnitude were observed experimentally for the reduction of *p*-benzoquinone by 10-methylacridan in the presence of substituted acetic acids.⁴⁷

Two different two-step mechanisms can also be excluded. Rapid and reversible hydride donation from ruthenium to the aldehyde carbonyl followed by proton transfer to the carbonyl oxygen can be excluded by the absence of deuterium exchange between PhCDO and siloxycyclopentadienyl ruthenium hydride **12**. Similarly, rapid and reversible protonation of the aldehyde carbonyl followed by hydride transfer from ruthenium appears unlikely because specific acid catalysis is normally accompanied by an inverse isotope effect.⁴²

Though concerted hydrogen transfer is the most economical mechanistic explanation for observation of isotope effects at

(41) Bullock, R. M. In *Transition Metal Hydrides*; Dedieu, A., Ed.; VCH: New York, 1992; Chapter 8, pp 263–307.

(42) Jencks, W. P. *Catalysis in Chemistry and Enzymology*; Dover: Mineola, NY, 1987; Chapter 4, pp 243–282.

(43) Noyori has reported an isotope effect of 1.5 ± 0.1 for dehydrogenation of 2-propanol by the 16 e⁻ precursor to **1**.^{2b}

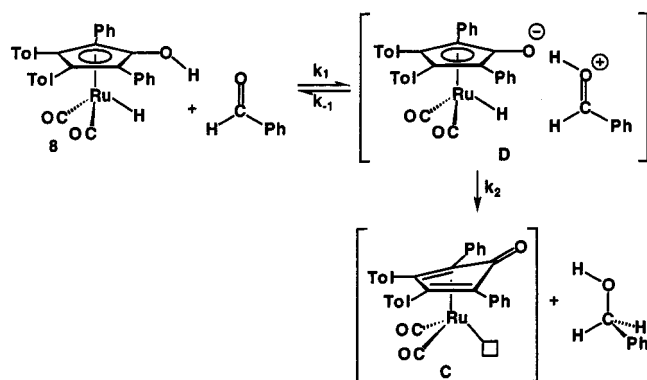
(44) For background on dehydrogenase enzymes, see: Abeles, R. H.; Frey, P. A.; Jencks, W. P. *Biochemistry*; Jones and Bartlett: Boston, 1992; Chapter 16, pp 447–477.

(45) (a) Wilkie, J.; Williams, I. H. *J. Am. Chem. Soc.* **1992**, *114*, 5423. (b) Wilkie, J.; Williams, I. H. *J. Chem. Soc., Perkin Trans. 2* **1995**, 1559.

(46) Coleman, C. A.; Rose, J. G.; Murray, C. J. *J. Am. Chem. Soc.* **1992**, *114*, 9755.

(47) The small isotope effects were rationalized by the coupling of heavy atom motion to proton transfer.^{45,46} Though the concerted transfers from **8** differ from these model system because the proton and hydride are electronically coupled, the small observed isotope effects may also be due to extensive heavy atom motion (lengthening of the carbonyl C–O bond and slippage of the η⁵-hydroxy-cyclopentadienyl ligand to an η⁴-cyclopentadienone ligand). Analysis of primary kinetic isotopes on hydrogen transfer in complexes related to **8** and analysis of heavy atom isotope effects will afford a more detailed picture of the transition state for concerted transfer.

Scheme 14



both centers, a stepwise mechanism in which the barriers for proton transfer followed by hydride transfer are approximately equal ($k_{-1} \approx k_2$ in Scheme 14) cannot be excluded. If k_{-1} and k_2 differ by a factor of 10 or greater, then an isotope effect would be seen only for the slower step. In this mechanism, endothermic proton transfer from oxygen is followed by fast hydride transfer from ruthenium. This hydride transfer must be extremely fast to have the same barrier as the exothermic back proton transfer between the aldehyde oxygen and the oxygen on the Cp ring. Such exothermic proton transfers between oxygen centers occur at near diffusion controlled rates.⁴⁸

For a concerted mechanism, the product of the individual isotope effects $\{(k_{\text{OHRuH}}/k_{\text{ODRuH}}) \times (k_{\text{OHRuH}}/k_{\text{OHRuD}}) = 2.2 \pm 0.1 \times 1.5 \pm 0.2 = 3.3 \pm 0.5\}$ should be equal to the isotope effect observed for doubly labeled material ($k_{\text{OHRuH}}/k_{\text{ODRuD}} = 3.6 \pm 0.3$). Within experimental error, this is the result observed. For the two-step mechanism shown in Scheme 14, the isotope effect observed for doubly labeled material should be smaller than the product of the individual isotope effects. For example, assuming no equilibrium isotope on formation of the protonated carbonyl intermediate and equal barriers for OH and RuH transfer, one must employ isotope effects of 3.4 on OH transfer and 2.0 on RuH transfer to obtain the observed isotope effects of $k_{\text{OHRuH}}/k_{\text{ODRuH}} = 2.2 \pm 0.1$ and $k_{\text{OHRuH}}/k_{\text{OHRuD}} = 1.5 \pm 0.2$ (see Supporting Information, pp 70–74). The combination of the two isotope effects predicts an isotope effect for double-labeled material of $k_{\text{OHRuH}}/k_{\text{ODRuD}} = 2.7$, which is smaller than the observed value of 3.6 ± 0.3 , but not far outside of error estimates. If we assume equal barriers for OH and RuH transfer and an equilibrium isotope effect of 1.5 favoring aldehyde protonation by **8** compared with aldehyde deuteration by **8-OD**, one must employ kinetic isotope effects of 3.0 on OH transfer and 2.0 on RuH transfer to obtain the observed isotope effects (see Supporting Information, pp 75–79).⁴⁹ This scheme then predicts an isotope effect for double-labeled material of $k_{\text{OHRuH}}/k_{\text{ODRuD}} = 3.0$. Again, this number is smaller than the observed 3.6 ± 0.3 , but not far outside of error estimates.

To distinguish between our favored concerted mechanism and a two-step mechanism with nearly equal barriers, we plan to investigate isotope effects on different substrates. For a two-step mechanism with a significantly different substrate, it is likely that one of the two steps will have a substantially different

barrier and an isotope effect will be seen at only one site. For concerted mechanisms, isotope effects should be seen for both steps even if the substrates are varied over a wide range.

The acidity of the Cp-OH ($\text{p}K_{\text{a}} = 17.5$ in CH_3CN) is crucial for successful hydride transfer from Ru-H. This hydroxyl group is more acidic than either phenol ($\text{p}K_{\text{a}} = 26.6$ in CH_3CN) or benzoic acid ($\text{p}K_{\text{a}} = 20.7$ in CH_3CN). When the acidic hydrogen was replaced by $-\text{SiEt}_3$ in compound **12**, no hydride transfer to PhCHO occurred. The anionic compound **13** with CpO^- is expected to be a better hydride donor than neutral **8**, but it proved to be unreactive toward PhCHO. The ability of **8** to transfer hydride from Ru clearly requires simultaneous proton transfer from CpO-H to the aldehyde oxygen. The small observed acceleration of PhCHO reduction in the presence of excess $\text{CF}_3\text{CO}_2\text{H}$ reinforces the importance of having the proton and hydride electronically coupled to achieve efficient hydrogen transfer.

The proposed concerted hydrogen transfer mechanism generates the coordinatively unsaturated dienone dicarbonyl intermediate **C** and free alcohol. Intermediate **C** was successfully trapped by PPh_3 and $\text{CF}_3\text{CO}_2\text{H}$. Though an alcohol complex may form transiently, it was not detected spectroscopically and probably does not play a role in hydrogen transfer. The absence of a detectable alcohol complex contrasts sharply with aldimine hydrogen transfer, in which a stable amine complex is formed after the transfer occurs.

Direct reductions by **8** require a polar multiple bond. The observations that cyclohexene does not react with **8** in the absence of H_2 and that reduction only occurs under H_2 suggests a very different mechanism for alkene reduction. We will address the mechanism of alkene reduction in detail in a future paper.

An alternative mechanism involves coordination of aldehyde to Ru followed by hydride transfer and requires prior CO dissociation (Scheme 4). Since the rate of reduction of PhCHO by **8** was not retarded under CO atmosphere, reversible CO dissociation can be excluded as a reaction step. Since ^{13}C exchange into **8** was much slower than the reaction of **8** with PhCHO, rate-determining CO loss can also be excluded as a reaction step. Rate-determining CO dissociation is also inconsistent with the observation of isotope effects and the second-order kinetics.

A ring-slip mechanism (Scheme 5) provides a route to aldehyde coordination without CO loss. If this mechanism were operative, then the triethylsiloxy ruthenium hydride **12** should be equally susceptible to ring slip, aldehyde coordination, and hydride transfer to give a Ru-O-CHDPh intermediate (Scheme 13). However, in the absence of an acidic proton the reduction would not be completed. The fact that PhCDO does not exchange with **12** is taken as evidence against the ring-slip mechanism. The observed isotope effects for reduction of PhCHO by **8** are not readily interpreted in terms of a ring-slip mechanism.

Comparison of Substrates. Hydrogen transfer from **8** to PhCHO occurs approximately 30 times faster than transfer to PhCOMe, consistent with the enhanced electrophilicity of the aldehyde. However, the $\text{MeN}=\text{CHPh}$ undergoes a more rapid hydrogen transfer than PhCHO, even though it has a more weakly polarized carbon-heteroatom bond. Since proton transfer of the acidic hydroxyl proton of **8** is crucial in promoting hydride transfer from Ru, the faster relative rate of $\text{MeN}=\text{CHPh}$ reduction may be attributed to the stronger basicity of the nitrogen heteroatom. The structure of the transition state for hydrogen transfer to $\text{MeN}=\text{CHPh}$ probably involves a larger degree of substrate protonation than in transfer to PhCHO.

(48) The diffusion-controlled rate is derived from Jencks' discussion of stepwise and concerted acid-base catalysis in aqueous solution and is intended as an estimate of the rate in organic solvents. (a) Jencks, W. P. *Acc. Chem. Res.* **1976**, *9*, 425. (b) Jencks, W. P. *Acc. Chem. Res.* **1980**, *13*, 161.

(49) The equilibrium between **8** + $\text{PhHC}=\text{OD}^+$ and **8-OD** + $\text{PhHC}=\text{OH}^+$ should favor deuterium at the site with the strongest bond, **8-OD**. Wiberg, K. B. *Physical Organic Chemistry*; John Wiley and Sons: New York, 1964; Part II, Chapter 7, pp 273–278.

Comparison with Other Metal Hydride Catalysts. As noted in the introduction, a number of metal complexes that contain both a metal hydride and an acidic proton on a coordinated ligand have recently been shown to be catalysts for transfer hydrogenation of ketones. These catalysts may well be mechanistically related to **8**. The reactivity of Noyori's Ru(II)-TsDPEN catalyst **1** (Scheme 1) resembles that of **8**. Both catalysts transfer hydrogen reversibly to carbonyl substrates, and the presence of an acidic proton on a coordinated ligand is crucial for efficient hydrogen transfer.²⁴ Though no detailed kinetic studies of the reduction of carbonyls by **1** have been reported, extensive computational studies have established that the concerted hydrogen transfer from **1** to ketones has a lower activation barrier than routes involving substrate coordination to the metal center followed by hydride transfer.⁵⁰

Hydrogen transfer to imines provides a striking reactivity difference between **8** and **1**. Hydrogen transfer from **8** is faster to imines than to ketones, while **1** reduces ketones but is unreactive toward imines.⁵¹ Calculations show that the activation barrier for hydrogen transfer from **1** to an imine is 5–11 kcal mol⁻¹ higher than the barrier for hydride transfer to carbonyls. This difference in relative reactivities may be accounted for by the more acidic pK_a of the OH group of **8** compared with that of the NH₂ group of **1**.

Comparison to Neutral Hydrides in the Presence of Strong Acids. Hydroxy-hydride **8**, which incorporates both acidic and hydridic hydrogens in the same molecule, may be compared to the reduction systems in which hydride and proton are delivered from separate molecules.⁵² Bullock and Norton found that the neutral transition metal hydrides, CpW(CO)₃H and CpMo(CO)₃H, reduced carbonyls to alcohols in the presence of strong Bronsted acids (CF₃CO₂H, CF₃SO₂H). In the reduction of acetone by CpW(CO)₃H/CF₃SO₂H, the alcohol complex [Cp(CO)₃W(OHCH(CH₃)₂)] [OTf] (**16**) was isolated and characterized. Kinetic studies on the CpMo(CO)₃H/CF₃CO₂H reduction of acetone showed the rate-determining step in the reduction was hydride transfer to a protonated ketone.

The Bullock–Norton ionic carbonyl hydrogenations and the Shvo system both utilize an acidic proton to promote hydride transfer. In both cases, ketone reduction is kinetically favored over dihydrogen evolution. **8** and related transfer hydrogenation catalysts differ from the ionic hydrogenation systems in that the active catalyst is formed from relatively unreactive precursors (alcohols, H₂, HCO₂H) and transfers proton and hydride in concert, not stepwise. Presumably, having the proton and hydride electronically coupled allows the reduction to proceed with the less acidic –OH proton in **8**. The concerted mechanism has significant benefits in providing a mild method to reduce carbonyls with excellent chemoselectivity. Another difference between the Bullock–Norton ionic carbonyl hydrogenations and reductions by **8** is that alcohol complexes such as **16** are isolated from the former system but no evidence for alcohol complexes was seen in reductions by **8**. The neutral intermediate **C** derived from hydrogen transfer from **8** binds alcohols poorly; this allows the catalyst to turn over without product alcohol inhibition.

(50) Yamakawa, M.; Ito, H.; Noyori, R. *J. Am. Chem. Soc.* **2000**, *122*, 1466.

(51) Under *catalytic* conditions, Noyori has reported that the Ru(II)-TsDPEN catalyst efficiently reduces imines to optically active amines with HCO₂H:NEt₃ (5:2) as the hydrogen source. The selectivity for imines over ketones is dramatic enough that the imine reductions may be run in acetone solvent. However, the observation that **1** is unreactive toward imines suggests that, under catalytic conditions, it is the protonated iminium ion that is reduced. Uematsu, N.; Fujii, A.; Hashiguchi, S.; Ikariya, T.; Noyori, R. *J. Am. Chem. Soc.* **1996**, *118*, 4916.

(52) Song, J. S.; Szalda, D. J.; Bullock, R. M.; Lawrie, C. J. C.; Rodkin, M. A.; Norton, J. R. *Angew. Chem., Int. Ed. Engl.* **1992**, *31*, 1233.

Relevance to Shvo Catalytic System. The kinetic studies of aldehyde reduction by **8** confirm Shvo's hypothesis that **8** is the active species in the catalytic reactions. Since the rate of stoichiometric reduction of PhCHO by **8** is so much faster than catalytic reduction, it is clear that regeneration of **8** after hydrogen transfer is the rate-determining step in the catalysis. In accord with this proposal, Shvo has shown by IR spectroscopy that the resting state in the catalytic reduction of cyclohexanone at 85 °C and 12 atm of H₂ is the diruthenium complex **3**.⁵³

Since the rate of reduction of PhCHO by **8** is so rapid, it should be possible to devise much more reactive catalysts by structural modifications that would prevent formation of the unreactive diruthenium species **6**. For example, increasing the steric bulk of the cyclopentadienone ligand might prevent the formation of diruthenium species but not greatly interfere with either the rate of regeneration of the hydroxy-hydride from H₂ or the rate of aldehyde reduction. We are exploring the synthesis of such complexes in the hope of developing highly active catalysts.

While the stoichiometric reduction of PhCHO by **8** is immeasurably faster than reduction of cyclohexene, Shvo has reported that cyclohexanone is catalytically reduced only eight times faster than cyclohexene. We are initiating detailed mechanistic investigations of alkene reduction by **8** to understand the underlying reasons for chemoselective reductions in both stoichiometric and catalytic systems.

Experimental Section

[2,5-Ph₂-3,4-Tol₂(η⁴-C₄CO)]Ru(CO)₃ (5**).** Ru₃(CO)₁₂ (400 mg, 0.62 mmol) and 2,5-diphenyl-3,4-(di-*p*-tolyl)cyclopenta-2,4-dien-1-one (**4**) (772 mg, 1.86 mmol) were dissolved in toluene (25 mL) and heated at reflux until the solution became light red (2–3 h).⁵⁴ The solution was concentrated to ~2 mL under vacuum and pentane (10 mL) was added to afford **5** (890 mg, 80%) as a pale yellow precipitate, which was collected by filtration, mp 164–166 °C dec. IR (CH₂Cl₂) 2083 (s), 2023 (br) cm⁻¹. ¹H NMR (C₆D₆, 300 MHz) δ 1.82 (s, 6H, tolyl CH₃), 6.62 (d, ³J = 8.0 Hz, 4 H, tolyl), 7.02 (m, 10 H, phenyl and tolyl), 7.94 (m, 4H, phenyl). ¹³C{¹H} NMR (C₆D₆, 75 MHz) δ 20.9 (CH₃), 81.5 (C 3,4 of Cp), 108.4 (C 2,5 of Cp), 127.2–138.5 (8 resonances, aromatic), 174.8 (C1 of Cp), 195.5 (CO). HRMS (EI) calcd (found) for C₃₄H₂₄O₄-Ru: 598.0711 (598.0699).

[2,5-Ph₂-3,4-Tol₂(η⁵-C₄CO)]₂H}Ru₂(CO)₄(μ-H) (6**).** Ru₃(CO)₁₂ (300 mg, 0.46 mmol) and **4** (578 mg, 1.40 mmol) were suspended in methanol (60 mL) and heated at reflux for 40 h. A bright yellow precipitate **6** (465 mg, 59%) was collected by filtration, mp 200–204 °C dec. IR (CH₂Cl₂) 2036 (vs), 2004 (m), 1977 (s) cm⁻¹. ¹H NMR (C₆D₆, 300 MHz) δ -17.68 (s, RuHRu), 1.79 (s, 12H, tolyl CH₃), 6.58 (d, ³J = 8.4 Hz, 8 H, tolyl), 6.95 (m, 12 H, phenyl), 7.09 (d, ³J = 8.4 Hz, 8 H, tolyl), 7.50 (m, 8 H, phenyl), 12.90 (br s, OH). ¹³C{¹H} NMR (C₆D₆, 75 MHz) δ 20.9 (CH₃), 88.2 (C 3,4 of Cp), 104.2 (C 2,5 of Cp), 127.0–137.8 (8 resonances, aromatic), 155.3 (C1 of Cp), 202.0 (CO). Anal. Calcd for C₆₆H₅₀O₆Ru₂: C, 69.46; H, 4.41. Found: C, 69.56; H, 4.31.

[2,5-Ph₂-3,4-Tol₂(η⁴-C₄CO)]Ru₂(CO)₂ (7**).** Ru₃(CO)₁₂ (531 mg, 0.83 mmol) and **4** (957 mg, 2.49 mmol) were suspended in heptane (175 mL) and heated at reflux for 48 h. The mustard yellow precipitate was collected by filtration to give **7** (1.04 g, 74%), mp 195–200 °C dec. IR (CH₂Cl₂) 2019 (s), 1967 (s) cm⁻¹. ¹H NMR (C₆D₆, 300 MHz) δ 1.69 (s, 12H, tolyl CH₃), 6.49 (d, ³J = 8.1 Hz, 8 H), 6.88 (m, 20 H, tolyl and phenyl), 7.50 (m, 8 H, phenyl). ¹³C{¹H} NMR (C₆D₆, 75 MHz) δ 20.8 (CH₃), 88.1 (C 3,4 of Cp), 99.2 (C 2,5 of Cp), 126.4–137.4 (8 resonances, aromatic), 171.5 (C1 of Cp), 200.8 (CO). Anal. Calcd for C₆₆H₄₈O₆Ru₂: C, 69.58; H, 4.24. Found: C, 69.82; H, 4.12.

(53) Blum, Y.; Czarkie, D.; Rahamim, Y.; Shvo, Y. *Organometallics* **1985**, *4*, 1459.

(54) It is crucial during the reflux to keep the oil bath temperature below 130 °C to prevent product decomposition.

[2,5-Ph₂-3,4-Tol₂(η^5 -C₄COH)]Ru(CO)₂H (8). A solution of **6** (20 mg, 0.02 mmol) in THF-*d*₈ (0.45 mL) in a resealable NMR tube was degassed by three successive freeze–pump–thaw cycles and placed under 1 atm of H₂ at –78 °C. The tube was sealed at –78 °C and heated at 80 °C in a constant-temperature bath for 8 h. The ¹H NMR spectrum of the yellow-orange solution showed >98% conversion to **8**. No isolation was attempted. IR (THF) 2012 (s), 1951 (s) cm⁻¹. ¹H NMR (THF-*d*₈, 500 MHz) δ -9.76 (s, RuH), 2.17 (s, 6H, tolyl CH₃), 6.80 (d, ³J = 7.9 Hz, 4 H, tolyl), 6.96 (d, ³J = 7.9 Hz, 4 H, tolyl), 7.23 (m, 6 H, phenyl), 7.47 (m, 4 H, phenyl), 8.60 (br s, OH). ¹³C{¹H} NMR (THF-*d*₈, 126 MHz) δ 21.1 (CH₃), 92.2 (C 3,4 of Cp), 104.7 (C 2,5 of Cp), 127.9–137.5 (8 resonances, aromatic), 137.6 (C1 of Cp), 203.0 (CO).

8 was also synthesized from HCO₂H and **6**. HCO₂H (7 μ L, 0.20 mmol) was added via syringe under a stream of N₂ to a solution of **6** in THF-*d*₈ (0.45 mL, 0.04 M solution). The ¹H NMR spectrum showed no reaction at room temperature. After the solution was heated at 80 °C until gas evolution ceased (10 min), the ¹H NMR spectrum showed complete conversion to **8**.

[2,5-Ph₂-3,4-Tol₂(η^5 -C₄COH)]Ru(CO)₂(O₂CCF₃) (11). CF₃CO₂H (55 μ L, 0.90 mmol) was added via syringe to a CH₂Cl₂ (10 mL) solution of **7** (110 mg, 0.10 mmol). After 1 h, solvent was evaporated under vacuum and the residue was recrystallized from CH₂Cl₂/pentane to give **11** (112 mg, 85%) as an air-stable light green powder, mp 160–162 °C dec. IR (CH₂Cl₂) 2045 (s), 1995 (s) cm⁻¹. ¹H NMR (CD₂Cl₂, 300 MHz) δ 2.25 (s, 6H, tolyl CH₃), 6.10 (br s, OH), 6.89 (AA'BB', 8 H, tolyl), 7.40 (m, 10 H, phenyl). ¹³C NMR{¹H} (CD₂Cl₂, 125 MHz) δ 21.3 (CH₃), 86.9 (C 3,4 of Cp), 101.0 (C 2,5 of Cp), 114.9 (q, ¹J_{CF} = 189 Hz, CF₃), 126.0–139.3 (8 resonances, aromatic), 142.2 (C1 of Cp), 163.7 (q, ²J_{CF} = 36 Hz, CF₃CO₂), 198.0 (CO). Anal. Calcd for C₃₅H₂₅O₃RuF₃: C, 61.49; H, 3.68. Found: C, 61.15; H, 3.52.

[2,5-Ph₂-3,4-Tol₂(η^5 -C₄COSiEt₃)Ru(CO)₂H] (12). SiEt₃H (175 μ L, 1.09 mmol) was added via syringe to a CH₂Cl₂ (8 mL) solution of **7** (200 mg, 0.17 mmol). After 4 h, solvent was evaporated under vacuum and the resulting green oil was dissolved in hexane (3 mL), filtered, and cooled to –35 °C to give **12** as a moisture-sensitive green solid (93 mg, 40%), mp 125–127 °C dec. IR (CH₂Cl₂) 2015 (s), 1954 (s) cm⁻¹. ¹H NMR (C₆D₆, 300 MHz) δ -9.20 (s, RuH), 0.50 (q, ³J = 7.3 Hz, SiCH₂), 0.74 (t, ³J = 7.3 Hz, SiCH₂CH₃), 1.81 (s, 6H, tolyl CH₃), 6.62 (d, ³J = 8.0 Hz, 4 H, tolyl), 7.00 (m, 6 H, phenyl), 7.29 (d, ³J = 8.0 Hz, 4 H, tolyl), 7.70 (m, 4 H, phenyl). ¹³C{¹H} NMR (C₆D₆, 125 MHz) δ 5.3 (SiCH₂), 7.1 (SiCH₂CH₃), 21.2 (CH₃), 95.8 (C 3,4 of Cp), 105.3 (C 2,5 of Cp), 128.6–137.6 (8 resonances, aromatic), 134.1 (C1 of Cp), 203.1 (CO). HRMS (EI) calcd (found) for C₃₉H₄₀O₃RuSi: 686.1783 (686.1815).

NEt₄⁺[2,5-Ph₂-3,4-Tol₂(η^5 -C₄CO)Ru(CO)₂H]⁻ (13). KBEt₃H (550 μ L, 1.0 M in THF) was added via syringe to a solution of **5** (200 mg, 0.34 mmol) and NEt₄Br (70 mg, 0.34 mmol) in THF (8 mL) at –78 °C. The solution was stirred for 20 min at room temperature and 1 N NaOH (5 mL) solution was added to destroy excess borohydride. THF was evaporated under vacuum leaving an aqueous solution with a yellow-green precipitate. The precipitate was washed with water (3 \times 5 mL) and hexane (10 mL) to give **13** (180 mg, 77%) as an off-white air-sensitive powder. IR (THF) 1974 (s), 1910 (s) cm⁻¹. ¹H NMR (THF-*d*₈, 300 MHz) δ -9.68 (s, RuH), 1.09 (br t, ³J = 6.5 Hz, NCH₂CH₃), 2.15 (s, 6H, tolyl CH₃), 3.15 (q, ³J = 6.5 Hz, NCH₂CH₃), 6.71 (d, ³J = 7.4 Hz, 4 H, tolyl), 7.04 (m, 10 H, tolyl and phenyl), 7.58 (m, 4 H, phenyl). ¹³C{¹H} NMR (THF-*d*₈, 125 MHz) δ 7.8 (NCH₂CH₃), 21.4 (s, tolyl CH₃), 52.9 (NCH₂CH₃), 84.2 (C 3,4 of Cp), 102.8 (C 2,5 of Cp), 124.6–139.2 (8 resonances, aromatic), 171.0 (C1 of Cp), 207.5 (CO). MS (MALDI-TOF) calcd (found) for C₃₃H₂₅O₃Ru⁻ 571.1 (571.1).

Exchange of ¹³CO with 8. A solution of **8** (0.08 M) in THF-*d*₈ prepared from **6** and H₂ was degassed, cooled to –78 °C, and placed under ¹³CO (1 atm). The tube was warmed to room temperature and shaken frequently. After 15 min, the hydride resonance of **8** at δ -9.76 was flanked by a doublet satellite (²J_{CH} = 9.5 Hz); the integrated ratio of the central peak to the doublet was 4:1. After 1.5 h, two additional outer lines were observed due to a triplet; the integrated ratio of the central singlet:doublet:triplet was 1:1:0.2. The reaction was discontinued after 3 h (*t*_{1/2} for disappearance of unlabeled **8** was ~1.5 h). When the ¹³CO exchange experiment was repeated in the absence of light, no

new satellites were observed for the hydride resonance at δ -9.76 after 2 h.

pK_a Determination of –OH Proton of 8. Solvent was removed in vacuo from a THF solution of **8** prepared from **6** and H₂. The yellow oily residue was redissolved in CH₃CN (0.070 M solution) and NEt₃ (3.0 μ L, 0.072 M) was added via gastight syringe. An aliquot of the solution was syringed into a 0.099 mm CaF₂ IR cell. Two resonances at 2014 and 1954 cm⁻¹ are due to **8** and two at 1985 and 1920 cm⁻¹ are due to NEt₃H⁺[2,5-Ph₂-3,4-Tol₂(η^5 -C₄CO)Ru(CO)₂H]⁻ (**15**). The absolute concentrations of the two species were determined by obtaining the molar absorptivities of **8** and **15**. For **8**: 2014 (2895 M⁻¹ cm⁻¹) and 1954 cm⁻¹ (2650 M⁻¹ cm⁻¹). For **15**: 1985 (2108 M⁻¹ cm⁻¹) and 1920 cm⁻¹ (2108 M⁻¹ cm⁻¹).⁵⁵ From the molar absorptivities, the ratio of **8** to **15** was determined to be 1:3.6. By using the known pK_a of NEt₃ (pK_a = 18.5) and the observed equilibrium constant (*K*_{eq} = 12.2), a pK_a of 17.5 was determined for the –OH proton of **8**.

Kinetics of PhCHO Reduction by 8. General procedure: PhCHO was added via gastight syringe under a stream of N₂ to a resealable NMR tube containing a THF-*d*₈ solution of **8** (0.05–0.08 M) and ferrocene (internal NMR integration standard) at –78 °C. The tube was evacuated and nitrogen readded. The tube was inserted into an NMR spectrometer precooled to –10 \pm 0.5 °C. The time between removal of the tube from the cold bath and acquisition of the first spectrum was ~3 min. The reactions were followed through 2–3 half-lives and the disappearance of **8** was measured by integrating its hydride resonance at δ -9.76 relative to ferrocene and plotting its disappearance with respect to time. All the kinetic runs were done with at least a 10-fold excess of PhCHO and followed pseudo-first-order kinetics. The products formed were PhCH₂OH and **6** as confirmed by ¹H NMR and GC.

[2,5-Ph₂-3,4-Tol₂(η^5 -C₄COD)]Ru(CO)₂D (8-d₂). After a suspension of **7** (15 mg, 0.013 mmol) in THF-*d*₈ (0.37 mL) under 1 atm of D₂ (added at –196 °C) was heated at 80 °C for 8 h, ¹H NMR indicated >98% conversion to **8-d₂** (0.07 M solution). The extent of deuteration at both the hydroxy and hydride positions was determined to be >90% by ¹H NMR comparison with the tolyl methyl resonance.

Deuterium Isotope Effect Measurements. A THF-*d*₈ solution of **8** (0.07 M), prepared from **6** and H₂, was degassed and PhCHO (47 μ L, 1.0 M) and D₂O (1.6 μ L, 0.2 M) were added at –78 °C. The tube was inserted into an NMR spectrometer precooled to 0 \pm 0.5 °C. The disappearance of the RuH ¹H NMR resonance was monitored over 3 half-lives: *k*_{obs} = 7.4 \times 10⁻⁴ s⁻¹; *t*_{1/2} = 15.6 min. In a second kinetic run, *k*_{obs} = 7.1 \times 10⁻⁴ s⁻¹ and *t*_{1/2} = 16.3 min. The products of the reaction were **6-OD** and PhCH₂OD.

Hydrogenation of Cyclohexene Catalyzed by 8 in THF. Cyclohexene (39 μ L, 0.38 mmol) was added via syringe to a THF-*d*₈ solution of **8** (0.09 M) prepared from **6** and H₂ at –78 °C. The solution was degassed and placed under H₂ (1 atm) at –78 °C. The tube was warmed to room temperature. No new resonances were observed by ¹H NMR after 30 min. After the solution was heated at 80 °C for 20 min, a new resonance was observed at δ 1.44, indicating cyclohexane formation. After 24 h, ~5 turnovers of cyclohexene had occurred.

X-ray Crystal Structure Determination for {[2,5-Ph₂-3,4-Tol₂(η^5 -C₄CO)]₂H}Ru₂(CO)₄(μ -H) (6). X-ray quality crystals were grown by cooling a CH₂Cl₂/hexane solution of **6** to –10 °C for one week. A yellow transparent plate-shaped crystal of dimensions 0.42 \times 0.36 \times 0.02 mm was selected for structural analysis. Intensity data for this compound were collected with a Bruker SMART CCD area detector mounted on a Bruker P4 goniometer using graphite-monochromated Mo K α radiation (λ = 0.71073 Å). The sample was cooled to 133(2) K. The intensity data, which nominally covered one and a half hemispheres of reciprocal space, were measured as a series of ϕ oscillation frames each of 0.4 ° for 60 s/frame. The detector was operated in 512 \times 512 mode and was positioned 5.00 cm from the sample. Coverage of unique data was 97.4% complete to 25.00° in θ . Cell parameters were determined from a nonlinear least-squares fit of 8192 peaks in the range 3.0 < θ < 25.0°. The first 50 frames were repeated at the end of data collection and yielded 224 peaks showing

(55) The molar absorptivities of the 1,1,3,3-tetramethylguanidinium salt **17** were used to determine the concentration of **15**. The CO stretches for **17** were observed at 1980 and 1915 cm⁻¹.

a variation of -0.02% during the data collection. A total of 29452 data were measured in the range $2.48 < \theta < 25.00^\circ$. The data were corrected for absorption by the empirical method⁵⁶ giving minimum and maximum transmission factors of 0.8129 and 0.9898. The data were merged to form a set of 11117 independent data with $R(\text{int}) = 0.0484$.

The triclinic space group $P\bar{1}$ was determined by statistical tests and verified by subsequent refinement. The structure was solved by direct methods and refined by full-matrix least-squares methods on F^2 .⁵⁷ Hydrogen atom positions were initially determined by geometry and were refined by using a riding model. Non-hydrogen atoms were refined with anisotropic displacement parameters. A total of 773 parameters were refined against 47 restraints and 11117 data to give $wR(F^2) = 0.1536$ and $S = 1.080$ for weights of $w = 1/[\sigma^2(F^2) + (0.0868P)^2 + 2.9570P]$, where $P = [F_o^2 + 2F_c^2]/3$. The final $R(F)$ was 0.0525 for the 8174 observed, $[F > 4\sigma(F)]$, data. The largest shift/s.u. was 0.049 in the final refinement cycle. The final difference map had maxima and minima of 1.207 and $-0.800 \text{ e}/\text{\AA}^3$, respectively.

X-ray Crystal Structure Determination for $\text{NEt}_4^+[\text{2,5-Ph}_2\text{-3,4-Tol}_2(\eta^5\text{-C}_4\text{CO})\text{Ru}(\text{CO})_2\text{H}]^-$ (13**).** X-ray quality crystals were grown by slow diffusion of hexane into a saturated THF solution of **13**. A yellow prism-shaped crystal of dimensions $0.38 \times 0.26 \times 0.06 \text{ mm}$ was selected for structural analysis. Intensity data for this compound were collected with a Bruker SMART CCD area detector mounted on a Bruker P4 goniometer using graphite-monochromated Mo $K\alpha$ radiation ($\lambda = 0.71073 \text{ \AA}$). The sample was cooled to 133(2) K. The intensity data, which nominally covered one and a half hemispheres of reciprocal space, were measured as a series of ϕ oscillation frames each of 0.4° for 20 s/frame. The detector was operated in 512×512 mode and was positioned 5.00 cm from the sample. Coverage of unique data was 91.2% complete to 25.00° in θ . Cell parameters were determined from a nonlinear least-squares fit of 4799 peaks in the range $2.54 < \theta < 26.89^\circ$. The first 50 frames were repeated at the end of

(56) Sheldrick, G. M. SADABS; Program for Empirical Absorption of Area Detector Data; University of Göttingen, Germany, 1996.

(57) Sheldrick, G. M. SHELXTL Version 5 Reference Manual. Bruker-AXS, 6300 Enterprise Dr., Madison, WI, 1994.

data collection and yielded 139 peaks showing a variation of 0.02% during the data collection. A total of 20519 data were measured in the range $1.99 < \theta < 25.00^\circ$. The data were corrected for absorption by the empirical method⁵⁵ giving minimum and maximum transmission factors of 0.662 and 0.942. The data were merged to form a set of 6772 independent data with $R(\text{int}) = 0.0560$.

The triclinic space group $P\bar{1}$ was determined by statistical tests and verified by subsequent refinement. The structure was solved by direct methods and refined by full-matrix least-squares methods on F^2 .⁵⁶ Hydrogen atom positions were initially determined by geometry and were refined with use of a riding model. Non-hydrogen atoms of the cation and anion were refined with anisotropic displacement parameters. A total of 481 parameters were refined against 21 restraints and 6772 data to give $wR(F^2) = 0.1895$ and $S = 1.036$ for weights of $w = 1/[\sigma^2(F^2) + (0.1240P)^2]$, where $P = [F_o^2 + 2F_c^2]/3$. The final $R(F)$ was 0.0650 for the 5106 observed, $[F > 4\sigma(F)]$, data. The largest shift/s.u. was 0.004 in the final refinement cycle. The final difference map had maxima and minima of 1.348 and $-0.920 \text{ e}/\text{\AA}^3$, respectively.

Acknowledgment. Financial support from the Department of Energy, Office of Basic Energy Sciences, is gratefully acknowledged. Steven Singer thanks the NIH (5T32 GM 08505) for support under a Chemistry Biology Interface Training Grant. Grants from NSF (CHE-9629688) and NIH (1 S10 RR04981-01) for the purchase of NMR spectrometers and from NSF (CHE-9105497) for the purchase of X-ray instruments are acknowledged.

Supporting Information Available: General experimental methods, experimental details, and characterization for **9**, **10**, and **14**, kinetics of reduction by **8**, and calculations of isotope effects and X-ray crystallographic data for **6**, **7**, **11**, and **13** (PDF). This material is available free of charge via the Internet at <http://pubs.acs.org>.

JA002177Z